

Ultraviolet-patterned acrylic pressure-sensitive adhesives for flexible displays

Jung-Hun Lee^{a,b}, Kyung-Min Kim^b, Hyun-Joong Kim^{b,c,*}, Youngdo Kim^{d,**}

^a Carbon Composite Materials Research Center, Korea Institute of Science and Technology, Jeonbuk, 55324, Republic of Korea

^b Laboratory of Adhesion and Bio-Composites, Department of Agriculture, Forestry and Bioresources, Seoul National University, Seoul, 08826, Republic of Korea

^c Research Institute of Agriculture and Life Sciences, Seoul National University, Seoul, 08826, Republic of Korea

^d Samsung Display Co, Ltd., Yongin, 17113, Republic of Korea

ARTICLE INFO

Keywords:

Acrylic pressure-sensitive adhesive

Ultraviolet patterning

Ultraviolet crosslinking

Adhesion

Recovery

Flexible display

ABSTRACT

Acrylic pressure-sensitive adhesives (PSAs) are extensively used to fasten display layers. Although PSAs must show sufficient adhesion for application to existing displays, PSAs must utilize stretching and recovery to mitigate the effects of deformation for application to flexible displays. Therefore, in this study, an ultraviolet (UV)-patterned acrylic PSA was prepared by incorporating a region showing variable degrees of crosslinking achieved using a contrasting UV-patterned film. The gel fraction was measured to confirm the degree of crosslinking, and the adhesion was measured by peel strength, pull-off, and lap shear tests. Dynamic mechanical analysis (DMA) stress relaxation was used to measure the recovery. The highest gel fraction was obtained at a crosslinker content of 1 part per hundred resin (phr) and a UV dose of 1600 mJ/cm². The low-crosslink-density area was optimized using the 50% gray patterned film. The acrylic PSA prepared with 0.001 phr of 2,5-bis(5-*tert*-butyl-benzoxazol-2-yl)thiophene (BBT), a light-emitting compound used to visualize the pattern formation, showed the clearest pattern. Although the adhesion of the UV-patterned acrylic PSA initially decreased, it gradually increased for the 2 mm pattern. However, the shear adhesion was maintained without appreciably changing. Although the acrylic PSA could not withstand certain deformation conditions during UV patterning, it was stretchable at a pattern size of 4 mm, and the recovery increased to approximately 60% at a pattern size of 2 mm. The results confirmed that the UV-patterned PSA is suitable for application to flexible displays.

1. Introduction

Acrylic-, silicon-, and rubber-based pressure-sensitive adhesives (PSAs) allow various materials to be assembled with only light pressure and attached without any residual water [1,2]. In particular, acrylic PSAs have attracted considerable attention in numerous industries because various reactive monomers can be selected and acrylic groups can be readily modified [3]. Although acrylic PSA is widely applied to assemble the layers used in various displays [4–8], the fourth industrial revolution currently underway is changing the way communications technology handles information, especially by providing consumers with customized services that intelligently combine controllable artificial intelligence with products that collect information. Therefore, displays have become increasingly important in machine–human

communication, which is competitively intensifying the development of flexible displays composed of a substrate (e.g., a window), a driving element (e.g., a thin-film transistor, (TFT)), a display element (e.g., a liquid-crystal display (LCD) or an organic light-emitting diode (OLED)), and an encapsulation, among other components, which must be able to bend freely. Currently, heterogeneous display materials may cause defects arising from bending-generated stress, and research is currently underway to solve this problem [9–19]. Recent work on PSAs has involved research on single-layer constituents for fixing and assembling flexible displays [20]. In addition, Simhadri et al. designed fluorinated bis-diazirines to manufacture flexible covalent adhesives that are as flexible as conventional polymer based adhesives. As an effective crosslinking agent, it exhibited an adhesion of more than 5 MPa to high density polyethylene (HDPE) with low surface energy [21]. Seo et al.

* Corresponding author. Laboratory of Adhesion and Bio-Composites, Department of Agriculture, Forestry and Bioresources, Seoul National University, Seoul, 08826, Republic of Korea.

** Corresponding author. ,

E-mail addresses: hjokim@snu.ac.kr (H.-J. Kim), colour.kim@samsung.com (Y. Kim).

<https://doi.org/10.1016/j.polymer.2021.124324>

Received 22 June 2021; Received in revised form 27 October 2021; Accepted 31 October 2021

Available online 2 November 2021

0032-3861/© 2021 Elsevier Ltd. All rights reserved.

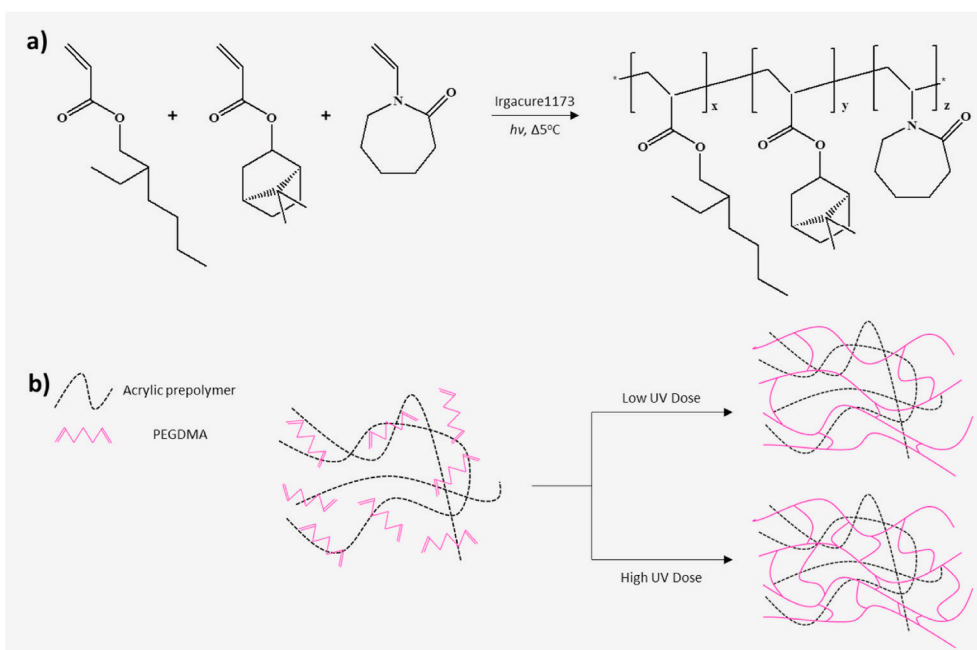


Fig. 1. Ideal schematic diagram. (a) Synthesis of acrylic prepolymer. (b) UV-dose-dependent crosslinking reactions.

reported a study on a multilayer flexible touch sensor. Multilayer flexible touch sensors were fabricated by printing parallel equidistance stripe pattern on PET film using conductive flexible adhesives (CFAs) as electrodes. CFAs are rubber based and have shown excellent performance in terms of flexibility, conductivity and durability. The critical pressure remained unchanged in each cell as the radius of curvature was decreased to 60 mm [22]. Kadioglu et al. reported a study on the behavior of flexible adhesives under the impact load of adhesive joints in automotive adhesive bonding. Flexible adhesives exhibit high strength and strain rates to improve structural impact resistance [23]. Son et al. reported a study on flexible shape memory polymer (SMP) adhesives. The advantage of SMP is that it adheres to harsh conditions such as underwater and rough surfaces. However, the disadvantages are that SMP is too hard to hold and strong adhesion to flexible surfaces. To improve this, they designed a flexible SMP adhesive composed of a backing fabric and a thin SMP layer [24]. To apply an acrylic PSA to a flexible display, the PSA must maintain sufficient adhesion to withstand deformation and recover when the deformation is released.

Previous studies have investigated various factors including the molecular weight, degree of crosslinking, type of elastomer, and reactive monomer composition used to develop PSAs for application to flexible displays [25–28]. The adhesion and recovery of acrylic PSAs were limited owing to the tradeoff between the molecular weight and crosslink density. Although elastomer-based acrylic PSAs show improved recoveries owing to relatively long molecular chains, it is difficult to

apply such PSAs to flexible displays because the adhesion exceeds the allowable limit.

As previously mentioned, the adhesion and recovery of acrylic PSAs are tradeoffs. That is, although low molecular weight and crosslink density are advantageous for PSA adhesion because of high wettability, they are disadvantageous for recovery owing to weak intermolecular interactions [25]. High molecular weight, crosslink density and monomer formulation, on the other hand, improve PSA recovery owing to the high degree of entanglement and the interaction between the molecular chains. However, because of the low degree of substrate interaction, the PSA adhesion deteriorates [26–29]. To overcome this tradeoff, an acrylic prepolymer was synthesized, and the ultraviolet (UV) radiation dose was adjusted to vary the pattern crosslink density (Fig. 1). The degree of PSA crosslinking was controlled by the UV dose and the contrast of the patterned film [30].

In this study, UV patterning was attempted in order to provide sufficient adhesion and recovery to withstand the stress and strain generated by the adhesive that fixes each layer when the display is folded or bent for flexible display application. Therefore, we observed the patterns formed by varying the crosslinker content and UV dose to optimize the low-crosslink-density region. In addition, UV-patterned acrylic PSAs were produced with various pattern sizes and were subsequently visualized. Fig. 2 shows the strategy for designing the UV-patterned acrylic PSAs. The low-crosslink-density region maintained adhesion by increasing the wettability. The high-crosslink-density region improved

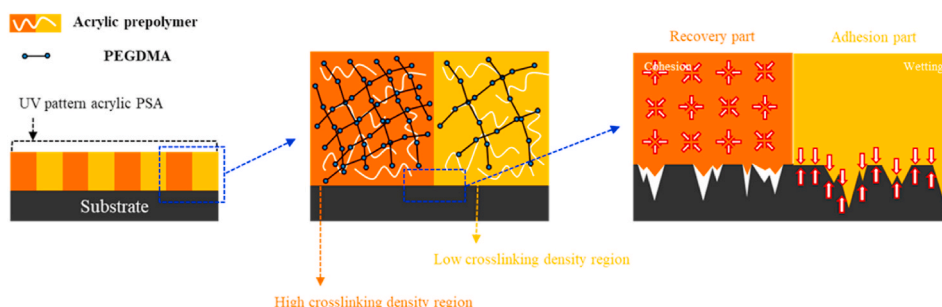


Fig. 2. Strategy for designing UV-patterned acrylic PSAs.

Table 1
Formulation of acrylic prepolymer.

Formulation	Acrylic prepolymer	
Reactive monomer (wt.%)	2-EHA	75
	IBA	21
	NVC	4
Phtoinitiator (phr)	Irgacure1173	1

Table 2
Formulation of UV crosslink acrylic PSAs.

Sample Names	Acrylic prepolymer* (wt. %)	Irgacure1173 (phr)	PEGDMA (phr)	UV Dose (mJ/cm ²)
PSA00	100	1	0	200–2400
PSA02			0.2	
PSA04			0.4	
PSA06			0.6	
PSA08			0.8	
PSA10			1.0	

Acrylic prepolymer* (WINNERSCHEM, Republic of Korea).

the acrylic PSA recovery by increasing cohesion. The PSA adhesion and recovery were plotted as functions of pattern size to confirm the applicability of the UV-patterned acrylic PSAs to flexible displays.

2. Experimental

2.1. Materials

An acrylic prepolymer (WinnersChem, Republic of Korea) was used as a general-purpose PSA without further purification to confirm the formation of a UV pattern showing a different crosslink density. Acrylic reactive monomers 2-ethylhexyl acrylate (2-EHA, 99.0% purity), isobornyl acrylate (IBA, 99.0% purity), and *N*-vinylcaprolactam (NVC, 99.0% purity) purchased from Samchun Pure Chemical Co., Ltd. (Republic of Korea) were used without further purification to polymerize the acrylic prepolymer to confirm the effect of the UV pattern on the PSA adhesion and recovery. Poly(ethylene glycol) dimethacrylate (PEGDMA, Sartomer, USA) and 2,5-bis(5-*tert*-butyl-benzoxazol-2-yl)thiophene (BBT, Sigma Aldrich, USA) were used as a crosslinker and luminescent

compound to visualize the PSA UV patterns, respectively. The photoinitiator used for the prepolymer polymerization and crosslinking was 2-hydroxy-2-methyl-1-phenyl-propan-1-one (Irgacure 1173, BASF, Germany).

2.2. Synthesis of acrylic prepolymer

The acrylic prepolymer was prepared by the bulk polymerization of the acrylic-monomer mixture, 2-EHA, IBA, and NVC by UV irradiation [4,31,32]. The mixture and the photoinitiator were charged into a dry 500 mL round-bottomed flask equipped with a four-necked separable flask and a mechanical stirrer, thermometer, and condenser with a drying tube and a N₂ inlet (Table 1). The mixture was steadily stirred for 20 min at room temperature in N₂ to remove the any residual oxygen, which retards the polymerization. The monomer mixture was synthesized by irradiation with a UV spot-cure system (SP-9, USHIO, Japan) under a N₂-rich atmosphere until the temperature of the mixture rose to 5 °C. The polymerization was iterated 5 times, and the acrylic prepolymer was stored in a wide-mouthed bottle to protect the prepolymer from light and air.

2.3. UV crosslinking of acrylic PSAs

The UV-crosslinked acrylic PSAs were prepared by blending 100 wt% of the synthesized acrylic prepolymer with 1 part per hundred of resin (phr) of PEGDMA and Irgacure 1173, respectively to obtain optimum crosslinking density. The mixture syrup was mixed and deformed using a paste mixer (SR-500, Thinky, Japan) for 2 min at 800 rpm. Subsequently, the acrylic PSA used to visualize the patterns was prepared by adding BBT to the blends, which were coated onto the surface of 75 μm-thick corona-treated polyethylene terephthalate (PET) films and covered with a silicone release film. In this step, the pattern film was covered over the silicone release films when the UV-patterned acrylic PSAs were prepared. The coated acrylic PSA films were then UV-crosslinked using conveyor-belt-type UV-crosslinking equipment operating with a 100 W high-pressure mercury lamp (main wavelength: 340 nm) [33]. To confirm the crosslink density of the acrylic PSAs, films were prepared using various crosslinker contents and UV doses (Table 2).

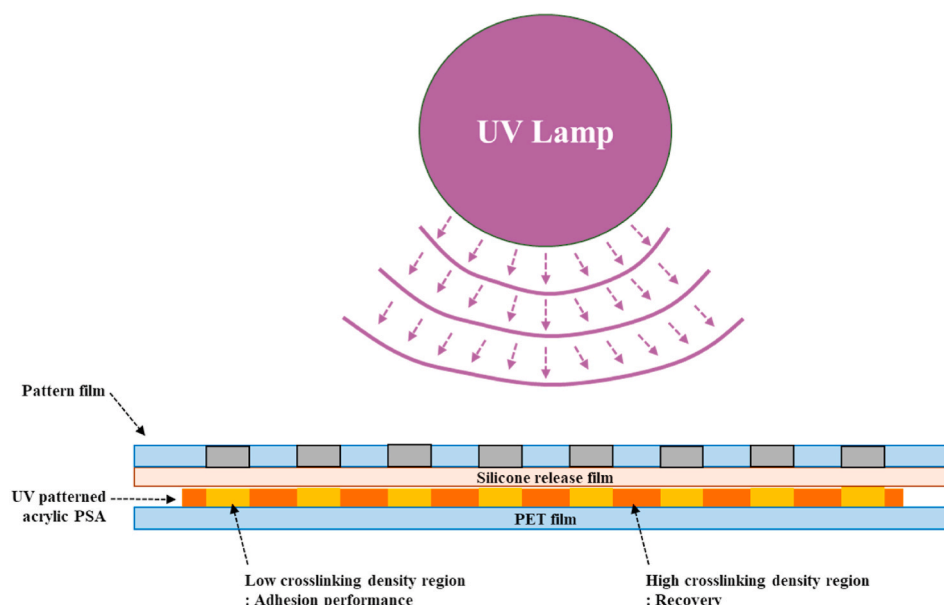


Fig. 3. Manufacturing of UV-patterned acrylic PSAs.

Table 3
Formulation of UV patterned acrylic PSAs for visualization.

Sample Names	Acrylic prepolymer* (wt.%)	Irgacure1173 (phr)	PEGDMA (phr)	BBT (phr)
PSA/BBT03	100	1	1	0.0003
PSA/BBT05				0.0005
PSA/BBT07				0.0007
PSA/BBT10				0.001

Acrylic prepolymer* (WINNERSCHEM, Republic of Korea).

2.4. Design of UV-patterned acrylic PSAs

Similar to the procedure followed to UV-crosslink the acrylic PSAs, a syrup was mixed with the acrylic prepolymer, and the crosslinker and photoinitiator were coated on a PET film and covered with a silicone release film. The UV-patterned acrylic PSA was prepared by UV irradiation and covered an overhead projector (OHP) film on which the pattern had been printed (Fig. 3), because when the pattern was printed, high- and low-crosslink-density regions were formed, thereby enabling recovery and adhesion, respectively. Furthermore, the UV intensity and pattern formation were investigated based on the pattern contrast. From this result, the UV-patterned acrylic PSAs were manufactured with different pattern sizes.

2.5. Visualization of UV-patterned acrylic PSAs

To visualize the pattern of the UV-patterned acrylic PSAs, BBT was mixed with the acrylic prepolymer, crosslinker, and initiator, and was prepared by UV crosslinking. As shown in Table 3, the pattern formation was confirmed by changing the BBT content to confirm the optimal content required for pattern visualization. The patterns of the BBT-containing UV-patterned acrylic PSAs were confirmed using UV irradiation [34].

2.6. Gel fraction

The gel content depends on the solvent solubility. In this work, toluene was selected as the solvent. The gel fractions of the crosslinker-blended acrylic PSAs were determined by shaking the samples (approximately 5 g) in toluene for 1 day at 20–22 °C. The soluble fraction was then removed by filtration and dried at 80 °C to a constant weight. The gel fraction was calculated using the following equation:

$$\text{Gel fraction (\%)} = (W_1/W_0) \times 100, \quad (1)$$

where W_0 and W_1 are the weights before and after filtration, respectively [25].

2.7. Adhesion strengths

The peel strengths of the 25 mm-wide specimens were investigated using a texture analyzer (TA-T2i, Micro Stable Systems, UK). The specimens were pressed onto stainless steel (SUS) substrates by two passes of a 2 kg rubber roller and then aged at room temperature for 24 h. The peel strength (defined as the average force applied to a PSA specimen during debonding) was determined in accordance with the ASTM D3330 standard at 180° and 20 °C and a crosshead velocity of 300 mm/min. The average applied force (in N/25 mm) was recorded for six different runs. The pull-off test was performed using a universal testing machine (AllroundLine Z010, 2 kN load cell, Zwick, Ulm, Germany). On a poly-methyl methacrylate (PMMA) surface, the UV-patterned acrylic PSAs were loaded, covered crosswise with a glass slide (120 × 25 × 1 mm³), pressed with a 2 kg weight for 5 min, and then aged at room temperature

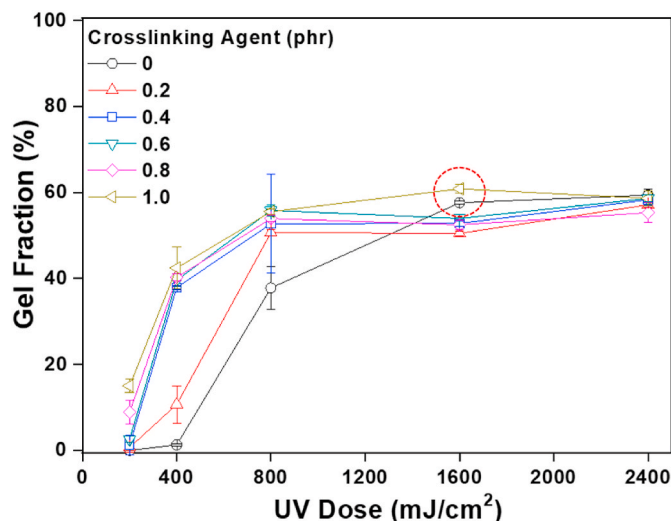


Fig. 4. Gel fraction plotted as functions of crosslinker content and UV dose.

for 24 h. The adhesion area was 25 × 25 mm², and the crosshead velocity was 5 mm/min. Lap shear was measured using a texture analyzer. The test specimens were cut into smaller 25 mm-wide pieces. Each PSA film removed from the silicone release film was attached to another PET substrate (the adhesion cross-sectional area was 25 × 25 mm², and a 2 kg rubber roller was passed over the film surface three times). Lap shear tests were performed at a crosshead velocity of 5 mm/min. The shear strains were calculated using the following equation:

$$\text{Shear strain (\%)} = \Delta L/t \times 100, \quad (2)$$

where ΔL is the moving distance and t is the PSA film thickness. The PSAs for application to flexible displays are usually subjected to different shear strains depending on the PSA structure and radius of curvature. Therefore, investigating the relationship between the shear strain rate and the thickness of the applied PSA films is imperative for their future application to flexible displays [25].

2.8. Recovery

The recovery of the UV-patterned acrylic PSAs was investigated by stress relaxation using a dynamic mechanical analysis (DMA) apparatus (Q-800 TA Instruments, USA) to determine the PSA characteristics and suitability for application to flexible displays by measuring the correlations between the deformation and stress with time. During the initial test, the PSA samples were stabilized for 1 min, and 300% strain was applied for 10 min. Afterwards, the test specimens were recovered for 5 min. The degrees of elastic recovery and residual creep strain were measured for the PSA samples and plotted as functions of time for different applied strains. The initial and final stresses and the relaxation ratios were determined from the obtained stress/time graphs [25].

3. Results and discussion

3.1. Gel fraction

To prepare the UV-patterned PSAs, the maximum degree of crosslinking allowed in the low-crosslink-density area must be determined based on the pattern contrast. Therefore, the gel fraction was measured based on the crosslinker content and the UV dose (Fig. 4). The gel fraction continuously increased with both increasing crosslinker content and UV dose (except for the crosslinker-free PSA) and stabilized above a UV dose of approximately 800 mJ/cm² because the C=C bonds available for the reaction were trapped between the polymer networks [35, 36]. In particular, when 1 phr of the crosslinker was added, the highest

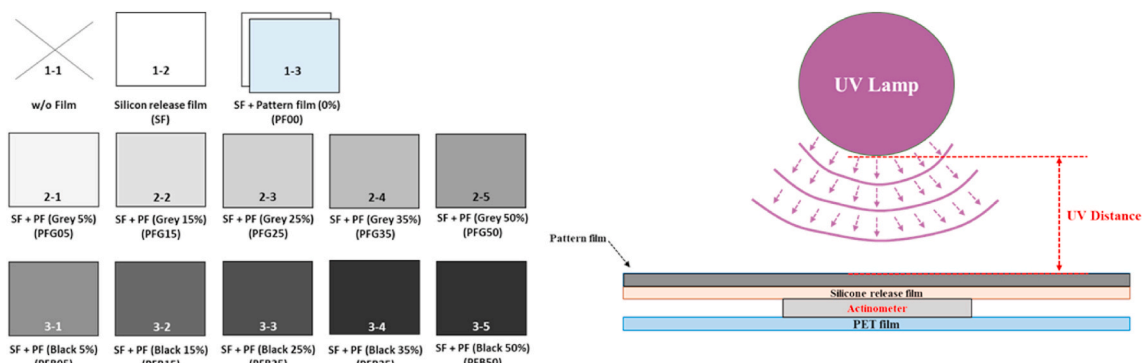


Fig. 5. Schematic showing pattern contrasts obtained for films patterned at various UV-irradiation distances.

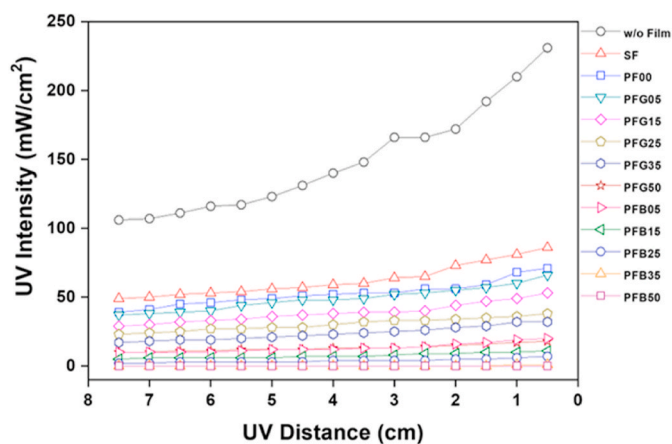


Fig. 6. UV intensity plotted as functions of pattern contrast and UV-irradiation distance.

gel fraction was obtained at a UV dose of 1600 mJ/cm² and was higher than that obtained at a UV dose of 2400 mJ/cm² because the crosslink rate also affects the crosslink density. In the low-crosslink-density area, the UV dose was inevitably low because the pattern was dark. However, because excessively low crosslinking impairs the PSA film reliability, the crosslinker content and UV dose should both be selected to maximize the degree of crosslinking. Therefore, the crosslinker content was fixed at 1 phr, and the UV dose was set to 1600 mJ/cm².

3.2. UV intensity

The low crosslinking density region of the UV-patterned acrylic PSA was formed by the pattern contrast, which, if too light, cannot form the pattern because the difference between the low- and high-crosslink-density regions is not distinct. If the contrast is too dark, on the other hand, the UV intensity is too low and sufficient crosslinking cannot be obtained. Therefore, to determine the optimal pattern contrast required for the low-crosslink-density area, the UV intensity was measured by adjusting the density of the pattern contrast and the distance between the PSA and the UV lamp (Fig. 5). Fig. 6 is a graph showing the UV

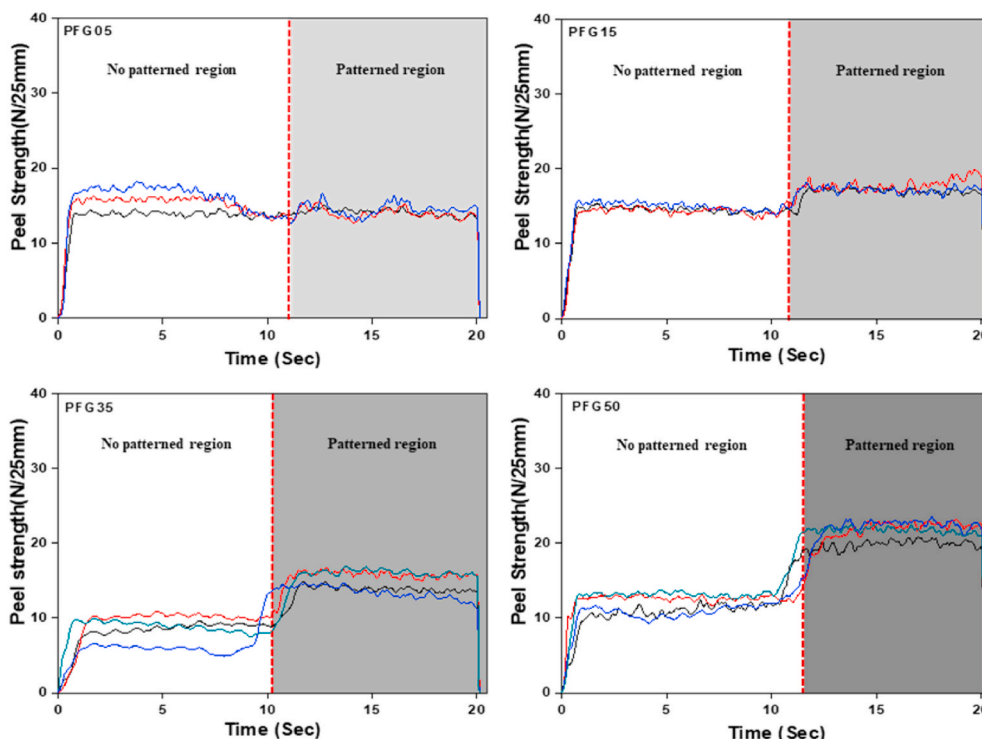


Fig. 7. Peel strength plotted as function of gray contrast intensity.

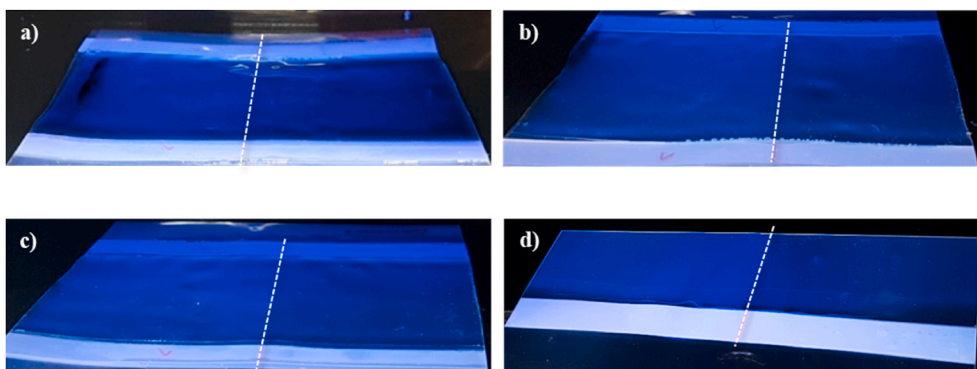


Fig. 8. Photographs of UV-patterned acrylic PSAs prepared with (a) 0.0003, (b) 0.0005, (c) 0.0007, or (d) 0.001 phr of BBT.

intensity plotted as functions of the pattern darkness and UV-irradiation distance. When the film was exposed, the UV intensity continued to increase to 240 mW/cm^2 with decreasing UV-irradiation distance. When a silicone film and a pattern film on which the pattern had not printed were added, the UV intensity rapidly decreased. As the pattern darkened, the UV intensity decreased continuously. In particular, for the black pattern, the UV intensity was approximately 0 mW/cm^2 . For the gray pattern, on the other hand, although the intensity sequentially decreased as the pattern darkened, the UV intensity stabilized in the range of approximately $18\text{--}66 \text{ mW/cm}^2$ when the UV-irradiation distance was 0.5 cm . The results suggest that the adhesion strength must be quantitatively measured based on the darkness of the gray pattern and the adhesion strength in the high-crosslink-density region.

3.3. Peel strength measured as function of contrast of gray pattern film

A sample was prepared and the peel strength was measured to confirm the pattern formed by the gray-pattern-induced formation of the low-crosslink-density region. Half of the gray pattern was printed on the pattern film used to prepare the PSA film, and the darkness of the gray pattern had changed. The prepared patterned film was then covered with the coated acrylic PSA film and irradiated with UV light. Fig. 7 shows the peel strength of the UV-patterned PSA plotted as a function of the gray-pattern contrast. The nonpatterned region of the PFG05 (Gray 5%) did not show any meaningful peel strength. From PFG15 (Gray

15%), a difference in peel strength emerged and increased with increasing pattern darkness. The difference between the peel strengths of the high- and low-crosslink-density areas of PFG15, PFG35, and PFG50 continued to rise to 2.4, 6.8, and 10.1 N/25 mm , respectively. Interestingly, the difference in the peel strength increased because not only did the peel strength of the low-crosslink-density region increase, but also that of the high-crosslink-density region decreased with increasing pattern thickness; this was attributed to the decrease in the UV dose of the low-crosslink-density region with increasing pattern darkness. Therefore, the diacrylate participates in the crosslinking, and the degree of crosslinking increases because it is concentrated in the nonpatterned acrylic prepolymer region. The graph in Fig. 7 shows that the difference between the adhesion strengths of the low- and high-crosslink-density regions was fixed at PEG50, which showed a difference of approximately 10 N/25 mm , and the UV-patterned acrylic PSA was studied based on this value.

3.4. Visualization of UV patterns as functions of BBT content and pattern size

Although the peel strength measurements confirmed that the patterns showed different degrees of crosslinking, BBT (a fluorescent dye) was used to more intuitively understand the pattern formation. To efficiently visualize the pattern, fluorescent dyes must be uniformly dispersed, and BBT is used for visualizing UV-patterned acrylic PSAs

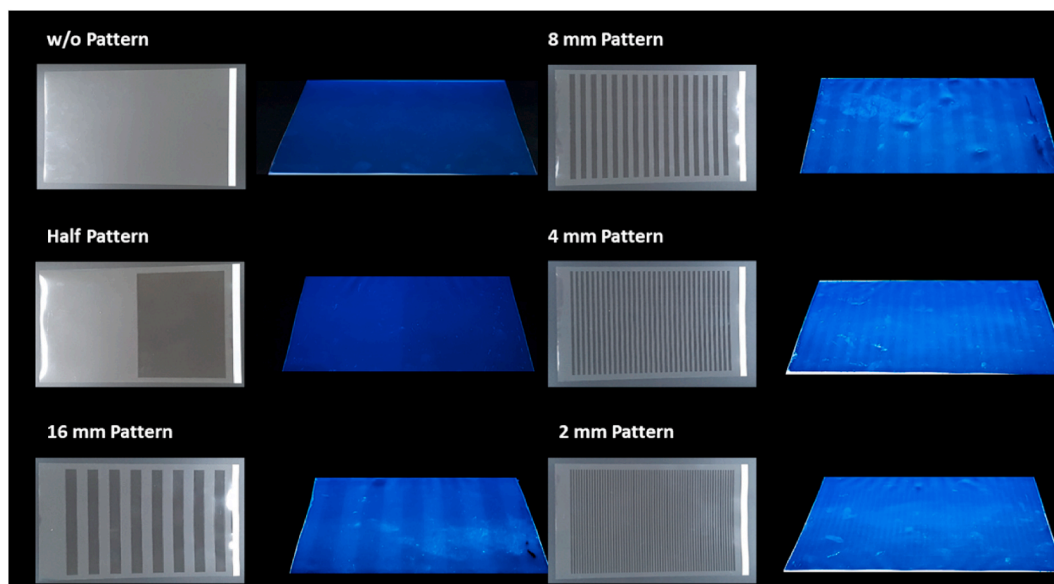


Fig. 9. Photographs of (a) nonpatterned, (b) half-patterned, and (c) 16, (d) 8, (e) 4, or (f) 2 mm UV-patterned acrylic PSAs.

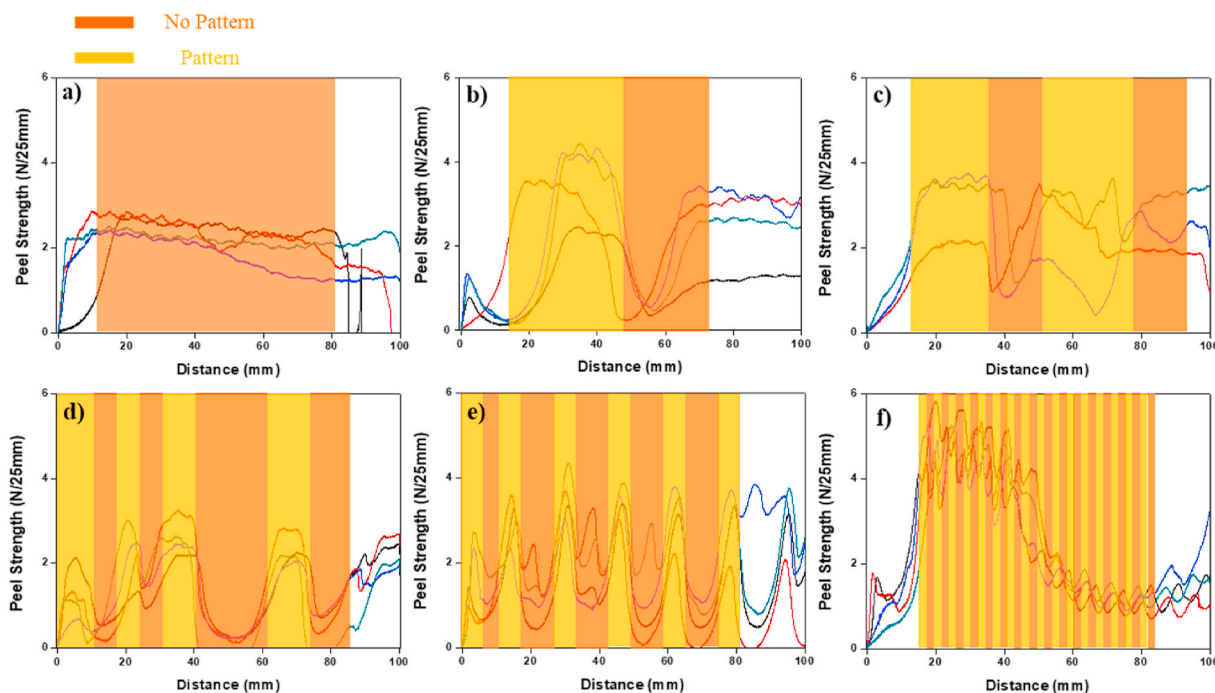


Fig. 10. Peel strength plotted as functions of pattern size for (a) nonpatterned, (b) half-patterned, and (c) 16, (d) 8, (e) 4, or (f) 2 mm UV-patterned acrylic PSAs.

because it belongs to a class of organic derivatives characterized by auxochrome groups and π -electron systems and shows very high solubility in various organic solvents. BBT absorbs light between 340 and 450 nm and fluoresces in the visible spectrum [37–40]. To optimize the BBT content, the UV-patterned acrylic PSA was visualized according to the BBT content. As shown in Fig. 8, as the BBT content increased, the difference between the low- and high-crosslink-density regions could be visualized under UV irradiation, and the difference was most pronounced at 0.001 phr. Therefore, the BBT content was fixed at 0.001 phr.

A patterned film was printed to determine how the degree of crosslinking affected the adhesion strength and recovery of the UV-patterned acrylic PSAs fabricated with various sizes of low- and high-crosslink-density areas. For an extreme comparison, nonprinted and half-printed pattern films were prepared, and the resulting pattern size reduced from 16 to 2 mm.

The concern in carrying out this experiment was that the pattern film may not play any role when the pattern size was reduced. Therefore, it would be difficult to discern the formation of a pattern showing a different degree of crosslinking because the difference in the UV-irradiation dose would be negligible. However, after the UV-irradiation patterning, the pattern was very well defined by the

visualization achieved using the BBT (Fig. 9). On the contrary, the UV-irradiation-induced crosslinking could be controlled very precisely.

3.5. Adhesion strength

The peel strength was measured to determine whether the UV-patterned acrylic PSAs actually showed different crosslink-density-dependent adhesion strengths (Fig. 10). Fig. 10a shows that the average peel strength was approximately 2.5 N/25 mm for the non-patterned crosslinked acrylic PSA. As the pattern was formed, the peel strengths of the patterned and nonpatterned regions started to differ. In addition, as the pattern size decreased, the frequency of fluctuations in the peel strength continuously increased in the region showing a different degree of crosslinking. As shown in Fig. 7, owing to the low-crosslink-density area, the crosslinking reaction was concentrated on the gray-pattern-free region and the crosslink density increased. In other words, when the pattern was formed, the peel strength of the high-crosslink-density region was lower than that of the counterpart region shown in Fig. 10a. Furthermore, the pattern-film-induced lower crosslink density was consistent with the initial UV pattern design with the intent to increase the adhesion strength.

It is difficult to quantitatively measure the adhesion strength of UV-

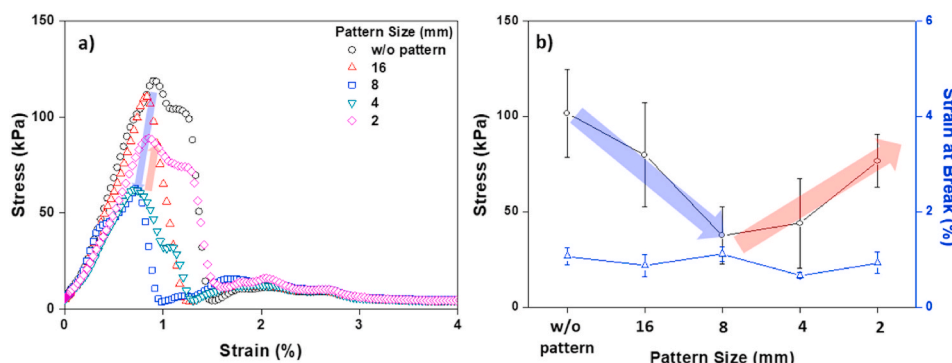


Fig. 11. Pull-off adhesion plotted as functions of pattern size for UV-patterned acrylic PSAs.

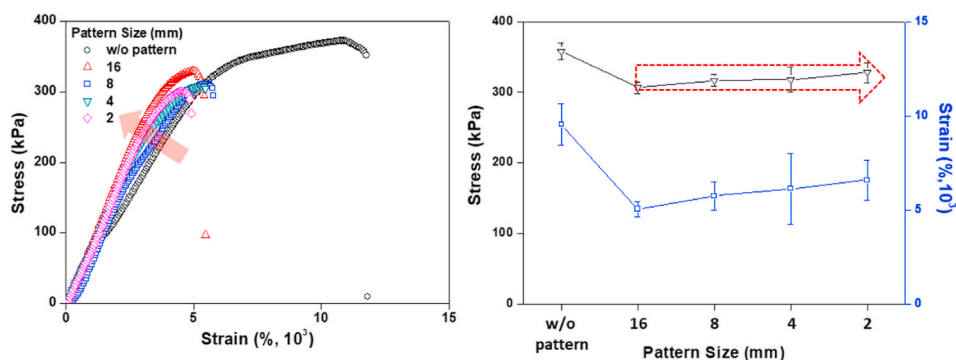


Fig. 12. Lap shear plotted as functions of pattern size for UV-patterned acrylic PSAs.

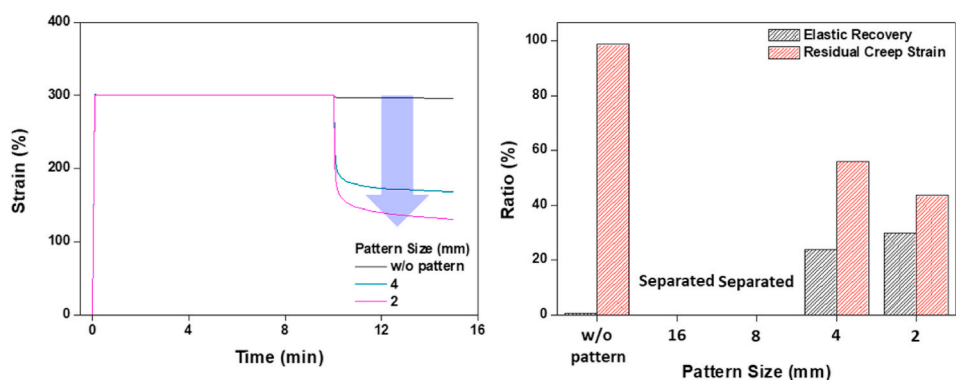


Fig. 13. Stress relaxation plotted as functions of pattern size for UV-patterned acrylic PSAs: (a) change in strain and (b) elastic recovery and residual creep strain.

patterned acrylic PSAs because the peel strength fluctuates according to the region. Therefore, a pull-off test was conducted to quantitatively evaluate the adhesion strength of the UV-patterned PSAs, and Fig. 11 shows the results. The adhesion strength continually decreased as the pattern was formed. Considering the peel strength measurements, although the adhesion strength should increase as the low-crosslink-density area is introduced, the coexistence of the low- and high-crosslink-density regions in the pull-off experiment showed that the adhesion strength actually had decreased by inhibiting the PSA cohesion itself. However, for the PSAs patterned at or below 8 mm, the adhesion strength began to increase, thereby confirming that the adhesion strength of the UV-patterned PSAs showing different degrees of cross-linking was reduced for a specific size. Therefore, a synergistic effect was observed when the pattern was densified.

Because the PSA shear adhesion is an essential factor in determining the applicability of the PSAs to flexible displays, a lap shear test was conducted to measure the shear adhesion (Fig. 12). Although the various

UV-patterned acrylic PSAs showed slightly decreased shear stress, there was no remarkable difference among the various pattern sizes. However, when the pattern was introduced, the shear strain rapidly decreased and the modulus slightly increased. Although decreasing the strain rate is disadvantageous for stretching, an increased modulus is beneficial for recovery. Therefore, it was necessary to determine how the patterning and pattern size affected the stretching and recovery by evaluating the latter.

3.6. Recovery

A stress relaxation test was conducted using DMA to confirm the stretching and recovery of the various UV-patterned acrylic PSAs. For the elongation analysis, 300% deformation was maintained for 10 min, and the recovery was analyzed after the deformation (Fig. 13). The nonpatterned acrylic PSAs were stretched by 300%, but hardly recovered after deformation. The 16 and 8 mm-patterned acrylic PSAs could

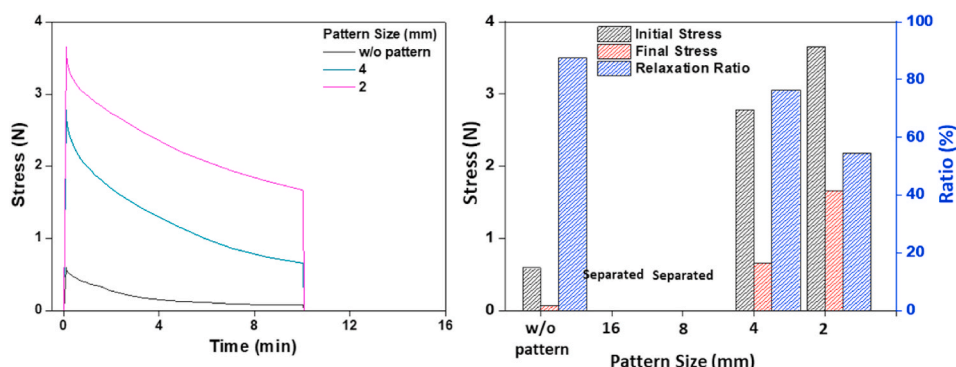


Fig. 14. Stress relaxation plotted as functions of pattern size for UV-patterned acrylic PSAs: (a) change in stress and (b) initial and final stresses and relaxation ratio.

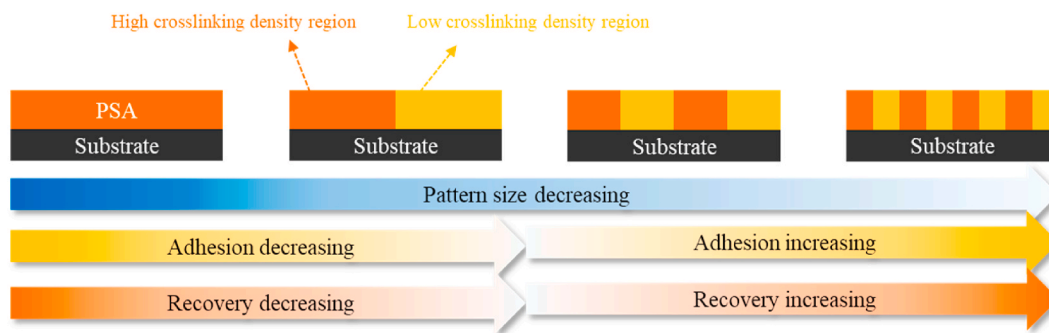


Fig. 15. Summary of pattern-size-based properties of UV-patterned acrylic PSAs.

not withstand 300% deformation, and the specimen was delaminated. In contrast, the 4 and 2 mm-patterned PSAs withstood the 300% deformation, and the recovery and elastic recoveries both increased. The elastic recovery of the 4 mm UV-patterned acrylic PSA was approximately 24%, the recovery after 4 min was approximately 44%, and the elastic recovery and the recovery of the 2 mm UV-patterned PSA increased to approximately 30% and approximately 60%, respectively, after 5 min because the PSA cohesion strength was adversely affected when the low-crosslink-density region was large. Furthermore, the synergy with the high-crosslink-density region increased when the low-crosslink-density region was small. Fig. 14 is a graph showing the stress generated when the UV-patterned acrylic PSAs were stretched by 300%. As in the strain-rate measurements, the 16 and 8 mm-patterned PSAs were delaminated, the initial/final stress of the 4 and 2 mm-patterned PSAs continuously increased, and the relaxation ratio decreased. When a material is deformed, the initial stress reflects the modulus of the material. That is, the modulus of the acrylic PSA increased with decreasing pattern size at or below 4 mm. The results of the lap shear test show that although the PSA modulus increased when the pattern was formed, there was no notable difference according to the pattern size. However, the results of stress relaxation showed that there was a subtle difference because the specimen substrate was different depending on the measurement method, and the rigid substrate used to measure the stress relaxation was more sensitive to the measurement than that used to measure only the PSA modulus. The results of this study confirm that the UV-patterned acrylic PSAs fabricated using pattern films showed improved adhesion strength and recovery when patterns showing different crosslinking degrees were densified (Fig. 15).

4. Conclusions

Overcoming the tradeoffs between the PSA degree of crosslinking, adhesion, and recovery, and combining the advantages of the high- and low-crosslink-density areas, we used a pattern film to prepare a UV-patterned acrylic PSA. The pattern formation was visualized using BBT, and the adhesion strength and the pattern-size-dependent stretching and recovery of the acrylic PSAs were systematically analyzed. However, although the adhesive cohesion strength itself inhibited the ability to combine the high- and low-crosslink-density regions, the adhesion synergistically increased and the shear modulus also improved when the pattern was densified to 8 mm or less. The stretching and recovery measurements suggest that when the low-crosslink-density area was large, the PSA could not stretch by 300% and was delaminated. However, when the pattern was reduced to 4 mm or less, the PSA not only could be stretched by 300% but also the recovery improved. In this study, although the pattern was only reduced to 2 mm, we will explore the feasibility of reducing the pattern to the micrometer regime and applying such PSAs to flexible displays in future studies.

CRediT authorship contribution statement

Jung-Hun Lee: Conceptualization, Methodology, Investigation, Writing – original draft. **Kyung-Min Kim:** Methodology, Investigation. **Hyun-Joong Kim:** Writing – original draft, Supervision, Funding acquisition. **Youngdo Kim:** Methodology, Visualization, Supervision.

Declaration of competing interest

The authors declare that they have no known competing financial interests or personal relationships that could have appeared to influence the work reported in this paper.

Acknowledgments

This work was financially supported by Samsung Display Co., Ltd., Republic of Korea.

References

- [1] D. Satas, *Handbook of Pressure-Sensitive Adhesive*, third ed., Technology, Van Nostrand-Reinhold, New York, 1999.
- [2] Z. Czech, R. Pelech, The thermal degradation of acrylic pressure-sensitive adhesives based on butyl acrylate and acrylic acid, *Prog. Org. Coating* 65 (1) (2009) 84–87, <https://doi.org/10.1016/j.porgcoat.2008.09.017>.
- [3] N. Ishikawa, M. Furutani, K. Arimitsu, Pressure-sensitive adhesive utilizing molecular interactions between thymine and adenine, *J. Polym. Sci., Part A: Polym. Chem.* 54 (10) (2016) 1332–1338, <https://doi.org/10.1002/pola.27977>.
- [4] C.-H. Park, S.-J. Lee, T.-H. Lee, H.-J. Kim, Characterization of an acrylic pressure-sensitive adhesive blended with hydrophilic monomer exposed to hygrothermal aging: assigning cloud point resistance as an optically clear adhesive for a touch screen panel, *React. Funct. Polym.* 100 (2016) 130–141, <https://doi.org/10.1016/j.reactfunctpolym.2016.01.012>.
- [5] J.-G. Lee, G.-S. Shim, J.-W. Park, H.-J. Kim, K.-Y. Han, Kinetic and mechanical properties of dual curable adhesives for display bonding process, *Int. J. Adhesion Adhes.* 70 (2016) 249–259, <https://doi.org/10.1016/j.ijadhadh.2016.07.005>.
- [6] E.P. Chang, D. Holguin, Curable optically clear pressure-sensitive adhesives, *J. Adhes.* 81 (5) (2005) 495–508, <https://doi.org/10.1080/00218460590944945>.
- [7] T. Wang, C.-H. Lei, A.B. Dalton, C. Creton, Y. Lin, K.S. Fernando, Y.-P. Sun, M. Manea, J.M. Asua, J.L. Keddie, Waterborne, nanocomposite pressure-sensitive adhesives with high tack energy, optical transparency, and electrical conductivity, *Adv. Mater.* 18 (20) (2006) 2730–2734, <https://doi.org/10.1002/adma.200601335>.
- [8] B.K. Ahn, S. Kraft, D. Wang, X.S. Sun, Thermally stable, transparent, pressure-sensitive adhesives from epoxidized and dihydroxyl soybean oil, *Biomacromolecules* 12 (5) (2011) 1839–1843, <https://doi.org/10.1021/bm200188u>, <https://www.ncbi.nlm.nih.gov/pubmed/21413679>.
- [9] Y. Leterrier, L. Médico, F. Demarco, J.-A.E. Månson, U. Betz, M.F. Escolà, M. Kharrazi Olsson, F. Atamny, Mechanical integrity of transparent conductive oxide films for flexible polymer-based displays, *Thin Solid Films* 460 (1–2) (2004) 156–166, <https://doi.org/10.1016/j.tsf.2004.01.052>.
- [10] P.C.P. Bouten, M.A.J. van Gils, Buckling failure of compressive loaded hard layers in flexible devices, *Mater. Res. Soc. Symp. Proc.* 843 (2005), <https://doi.org/10.1557/PROC-843-T4.9>, T4.9.1.
- [11] C.-J. Chiang, C. Winscom, S. Bull, A. Monkman, Mechanical modeling of flexible OLED devices, *Org. Electron.* 10 (7) (2009) 1268–1274, <https://doi.org/10.1016/j.orgel.2009.07.003>.
- [12] O. van der Sluis, R.A.B. Engelen, P.H.M. Timmermans, G.Q. Zhang, Numerical analysis of delamination and cracking phenomena in multi-layered flexible

- electronics, *Microelectron. Reliab.* 49 (8) (2009) 853–860, <https://doi.org/10.1016/j.microrel.2009.03.013>.
- [13] A.A. Abdallah, P.C.P. Bouten, J.M.J. den Toonder, G. De With, Buckle initiation and delamination of patterned ITO layers on a polymer substrate, *Surf. Coating Technol.* 205 (8–9) (2011) 3103–3111, <https://doi.org/10.1016/j.surfcoat.2010.11.025>.
- [14] O. van der Sluis, A.A. Abdallah, P.C.P. Bouten, P.H.M. Timmermans, J.M.J. den Toonder, G. de With, Effect of a hard coat layer on buckle delamination of thin ITO layers on a compliant elasto-plastic substrate: an experimental-numerical approach, *Eng. Fract. Mech.* 78 (6) (2011) 877–889, <https://doi.org/10.1016/j.engfractmech.2011.01.013>.
- [15] C.-C. Lee, Y.-S. Shih, C.-S. Wu, C.-H. Tsai, S.-T. Yeh, Y.-H. Peng, K.-J. Chen, Development of robust flexible OLED encapsulations using simulated estimations and experimental validations, *J. Phys. D Appl. Phys.* 45 (27) (2012), <https://doi.org/10.1088/0022-3727/45/27/275102>. <http://www.ncbi.nlm.nih.gov/pubmed/275102>. <http://stacks.iop.org/JPhysD/45/275102>.
- [16] C.-C. Lee, Modeling and validation of mechanical stress in indium tin oxide layer integrated in highly flexible stacked thin films, *Thin Solid Films* 544 (2013) 443–447, <https://doi.org/10.1016/j.tsf.2013.02.084>.
- [17] M.-K. Yeh, L.-Y. Chang, M.-R. Lu, H.-C. Cheng, P.-H. Wang, Bending stress analysis of flexible touch panel, *Microsyst. Technol.* 20 (8–9) (2014) 1641–1646, <https://doi.org/10.1007/s00542-014-2200-1>.
- [18] H.-C. Cheng, W.-H. Xu, W.-H. Chen, P.-H. Wang, K.-F. Chen, C.-C. Chang, Bending characteristics of foldable touch display panel with a protection structure design, *Ann. Mater. Sci. Eng.* 2015 (2015) 1–16, <https://doi.org/10.1155/2015/106424>. <http://www.ncbi.nlm.nih.gov/pubmed/106424>.
- [19] S. Li, Y. Su, R. Li, Splitting of the neutral mechanical plane depends on the length of the multi-layer structure of flexible electronics, *Proc. R. Soc. A* 472 (2016) 20160087, <https://doi.org/10.1098/rspa.2016.0087>, 2190.
- [20] F. Salmon, A. Everaerts, C. Campbell, B. Pennington, B. Erdogan-Haug, G. Caldwell, Modeling the mechanical performance of a foldable display panel bonded by 3M optically clear adhesives, *Dig. Tech. Pap. Soc. Inf. Disp. Int. Symp.* 48 (2017) 938–941, <https://doi.org/10.1002/sdtp.11796>, 64–1.
- [21] C. Simhadri, L. Bi, M.L. Lepage, M. Takaffoli, Z. Pei, S.F. Musolino, A.S. Milani, G. A. DiLabio, J.E. Wulff, Flexible polyfluorinated bis-diazirines as molecular adhesives, *Chem. Sci.* 12 (11) (2021) 4147–4153, <https://doi.org/10.1039/d0sc06283a>.
- [22] S. Seo, S. Kim, J. Jung, R. Ma, S. Baik, H. Moon, Flexible touch sensors made of two layers of printed conductive flexible adhesives, *Sensors* 16 (9) (2016) 1515, <https://doi.org/10.3390/s16091515>.
- [23] F. Kadioglu, R.D. Adams, Flexible adhesives for automotive application under impact loading, *Int. J. Adhesion Adhes.* 56 (2015) 73–78, <https://doi.org/10.1016/j.ijadhadh.2014.08.001>.
- [24] C. Son, S. Kim, Dual adaptation of a flexible shape memory polymer adhesive, *ACS Appl. Mater. Interfaces* 13 (23) (2021) 27656–27662, <https://doi.org/10.1021/acsaami.1c05434>.
- [25] J.-H. Lee, T.-H. Lee, K.-S. Shim, J.-W. Park, H.-J. Kim, Y. Kim, S. Jung, Molecular weight and crosslinking on the adhesion performance and flexibility of acrylic PSAs, *J. Adhes. Sci. Technol.* 30 (21) (2016) 2316–2328, <https://doi.org/10.1080/01694243.2016.1182382>.
- [26] J.-H. Lee, T.-H. Lee, K.-S. Shim, J.-W. Park, H.-J. Kim, Y. Kim, S. Jung, Effect of crosslinking density on adhesion performance and flexibility properties of acrylic pressure sensitive adhesives for flexible display applications, *Int. J. Adhesion Adhes.* 74 (2017) 137–143, <https://doi.org/10.1016/j.ijadhadh.2017.01.005>.
- [27] J.-H. Lee, G.-S. Shim, J.-W. Park, H.-J. Kim, Y. Kim, Adhesion performance and recovery of acrylic pressure-sensitive adhesives thermally crosslinked with styrene–isoprene–styrene elastomer blends for flexible display applications, *J. Ind. Eng. Chem.* 78 (2019) 461–467, <https://doi.org/10.1016/j.jiec.2019.05.019>.
- [28] J.H. Lee, J. Park, M.H. Myung, M.-J. Baek, H.-S. Kim, D.W. Lee, Stretchable and recoverable acrylate-based pressure sensitive adhesives with high performance, optical clarity, and metal corrosion resistance, *Chem. Eng. J.* 406 (2021) 126800, <https://doi.org/10.1016/j.cej.2020.126800>.
- [29] X. Zhang, Y. Ding, G. Zhang, L. Li, Y. Yan, Preparation and rheological studies on the solvent based acrylic pressure sensitive adhesives with different crosslinking density, *Int. J. Adhesion Adhes.* 31 (7) (2011) 760–766, <https://doi.org/10.1016/j.ijadhadh.2011.07.004>.
- [30] J.-H. Back, D. Baek, K.-B. Sim, G.-Y. Oh, S.-W. Jang, H.-J. Kim, Y. Kim, Optimization of recovery and relaxation of acrylic pressure-sensitive adhesives by using UV patterning for flexible displays, *Ind. Eng. Chem. Res.* 58 (10) (2019) 4331–4340, <https://doi.org/10.1021/acs.iecr.8b05208>.
- [31] Z. Czech, M. Wesolowska, Development of solvent-free acrylic pressure-sensitive adhesives, *Eur. Polym. J.* 43 (8) (2007) 3604–3612, <https://doi.org/10.1016/j.eurpolymj.2007.05.003>.
- [32] Z. Czech, R. Milker, Solvent-free radiation-curable polyacrylate pressure-sensitive adhesive systems, *J. Appl. Polym. Sci.* 87 (2) (2003) 182–191, <https://doi.org/10.1002/app.11303>.
- [33] S.-W. Lee, J.-W. Park, C.-H. Park, H.-J. Kim, Enhanced optical properties and thermal stability of optically clear adhesives, *Int. J. Adhesion Adhes.* 50 (2014) 93–95.
- [34] M.A. Fourati, T. Maris, W.G. Skene, C.G. Bazuin, R.E. Prud'homme, Photophysical, electrochemical and crystallographic investigations of the fluorophore 2,5-bis(5-tert-butyl-benzoxazole-2-yl)thiophene, *J. Phys. Chem. B* 115 (2011) 12362–12369, <https://doi.org/10.1021/jp207136k>.
- [35] H.-S. Joo, Y.-J. Park, H.-S. Do, H.-J. Kim, S.-Y. Song, K.-Y. Choi, The curing performance of UV-curable semi-interpenetrating polymer network structured acrylic pressure-sensitive adhesives, *J. Adhes. Sci. Technol.* 21 (7) (2007) 575–588, <https://doi.org/10.1163/156856107781192346>.
- [36] S.-W. Lee, T.-H. Lee, J.-W. Park, C.-H. Park, H.-J. Kim, J.-Y. Song, J.-H. Lee, Curing behaviors of UV-curable temporary adhesives for a 3D multichip package process, *J. Electron. Mater.* 43 (11) (2014) 4246–4254, <https://doi.org/10.1007/s11664-014-3354-4>.
- [37] R. Chen, J. Qu, Q. Zhao, J. He, Environmental impact on the light and perspiration stability of triazinylstilbene fluorescent brighteners on cotton fabrics, *Fibers Polym.* 15 (9) (2014) 1915–1920, <https://doi.org/10.1007/s12221-014-1915-z>.
- [38] Q. Zhao, J. Sun, B. Liu, J. He, Coloring properties of novel 1,4-distyrylbenzene and 4,4'-distyrylbiphenyl fluorescent brighteners and their arrangement in cotton and polyester fiber, *Cellulose* 21 (4) (2014) 2937–2950, <https://doi.org/10.1007/s10570-014-0260-0>.
- [39] R. Chen, J. Qu, D. Yang, J. He, Light and perspiration stability of triazinylstilbene fluorescent brighteners on cotton fabrics, *Textil. Res. J.* 84 (7) (2014) 772–782, <https://doi.org/10.1177/0040517513509869>.
- [40] X. Zuo, F. Morlet-Savary, B. Graff, N. Blanchard, J.P. Goddard, J. Lalevée, Fluorescent brighteners as visible LED-light sensitive photoinitiators for free radical photopolymerizations, *Macromol. Rapid Commun.* 37 (10) (2016) 840–844, <https://doi.org/10.1002/marc.201600103>. <https://www.ncbi.nlm.nih.gov/pubmed/27072016>.